J|A|C|S
ARTICLES
Published on Web 05/11/2007

Anion Chelation by Amido Acid Functionalized Fused Quartz/Water Interfaces Studied by Nonlinear Optics

Julianne M. Gibbs-Davis, Patrick L. Hayes, Karl A. Scheidt, and Franz M. Geiger*

Contribution from the Department of Chemistry and International Institute for Nanotechnology, Institute for Environmental Catalysis, Northwestern University, 2145 Sheridan Road, Evanston, Illinois 60208-3113

Received November 13, 2006; E-mail: geigerf@chem.northwestern.edu

Abstract: We report resonantly enhanced surface second harmonic generation (SHG) measurements to track the interaction of the EPA priority toxic metal pollutant chromium(VI) with fused quartz/water interfaces containing tailor-made amino acids that serve as model systems for environmental and biological interfaces. $\chi^{(3)}$ measurements of amido acid functionalized fused quartz/water interfaces are consistent with two acid−base equilibria, suggesting the formation of a laterally hydrogen-bonded environment similar to what is observed for aliphatic carboxylic acids. Chromate adsorption isotherms recorded at pH 7 are suggestive of an intramolecular chelation mechanism that becomes important when four or more hydrogen-bonding moieties are displayed toward the incoming chromate. The strong binding affinities of the amido acid functionalized fused quartz/water interfaces toward chromate are consistent with nearly 50% slower transport rates with respect to free-flowing groundwater, indicating that, in the absence of redox processes, peptide materials in heterogeneous geochemical environments can significantly increase chromate residence times. The strong evidence for synergistic effects dominating the interactions of chromate with surface-bound amido acids indicates that chemical complexity can be systematically addressed using tailor-made organic surfaces and interfaces.

1. Introduction

Tailor-made surfaces and interfaces are emerging as an exciting field of research in many areas of chemistry, including environmental and energy science, catalysis, materials science, and biology.[1−14] As an interdisciplinary group integrating the study of surface phenomena with synthetic chemistry, we have developed an amide-coupling approach[15,16] to generate multivalent and chemically robust heterogeneous systems with tunable chemical and physical properties. Specifically, we report how the functionalization of silica surfaces with amino acids can be used to bridge the complexity gap associated with studying environmental interfaces.

Environmental molecular science is a field that combines the traditional areas of organic, inorganic, physical, and analytical chemistry. Research in this new arena places a significant emphasis on experimental and theoretical studies of mineral oxide surfaces because of their abundance in geochemical[17,18] and atmospheric environments.[19,20] For instance, mineral oxide particles present in dust storms from the Sahara or Gobi desert are rich in silicates and related oxides and represent a very large cumulative surface area for heterogeneous chemistry that can occur for days.[21] Similarly, colloidal suspensions of mineral oxide particles as well as macroscopic mineral oxide/water interfaces are abundant in geochemical and aquatic environments.[22] In addition to mineral oxides, the ubiquity of polar and multifunctional oligomeric compounds produced from biodegradation or the metabolism of microbes and plants[23−25] increases the complexity of environmental interfaces to levels typically associated with biological systems.[26] The high level of complexity characteristic of these organic surfaces poses a significant challenge to catalog, predict, and control physico-

(1) Lahann, J.; Mitragotri, S.; Tran, T.-N.; Kaido, H.; Sundaram, J.; Choi, I. S.; Hoffer, S.; Somorjai, G.; Langer, R. *Science* **2003**, *299*, 371.
(2) Prime, K. J.; Whitesides, G. M. *Science* **1991**, *252*, 1164.
(3) Holden, M. A.; Jung, S.-Y.; Yang, T.; Castellana, E. T.; Cremer, P. S. *J. Am. Chem. Soc.* **2004**, *126*, 6512.
(4) Ikeura, Y.; Kurihara, K.; Kunitake, T. *J. Am. Chem. Soc.* **1991**, *113*, 7342.
(5) Lasseter, T. L.; Clare, B. H.; Abbott, N. L.; Hamers, R. J. *J. Am. Chem. Soc.* **2004**, *126*, 10220.
(6) Fresco, Z. M.; Frechet, J. M. J. *J. Am. Chem. Soc.* **2005**, *127*, 8302.
(7) Horvath, J. D.; Kortnik, A.; Kamakoti, P.; Sholl, D. S.; Gellman, A. J. *J. Am. Chem. Soc.* **2004**, *126*, 14988.
(8) Crespo-Biel, O.; Dordi, B.; Reinhoudt, D. N.; Huskens, J. *J. Am. Chem. Soc.* **2005**, *127*, 7594.
(9) Mann, D. A.; Kanai, M.; Maly, D. J.; Kiessling, L. L. *J. Am. Chem. Soc.* **1998**, *120*, 10575.
(10) Chance, J. J.; Purdy, W. C. *Langmuir* **1997**, *13*, 4487.
(11) Han, M. Y.; Kane, R.; Goto, M.; Belfort, G. *Macromolecules* **2003**, *36*, 4472.
(12) Hu, K.; Bard, A. J. *Langmuir* **1997**, *13*, 5114.
(13) Zhou, D. J.; Wang, X. Z.; Birch, L.; Rayment, T.; Abell, C. *Langmuir* **2003**, *19*, 10557.
(14) Burke, S. E.; Barrett, C. J. *Langmuir* **2003**, *19*, 3297.
(15) Boman, F. C.; Musorrafiti, M. J.; Gibbs, J. M.; Stepp, B. R.; Salazar, A. M.; Nguyen, S. T.; Geiger, F. M. *J. Am. Chem. Soc.* **2005**, *127*, 15368.
(16) Voges, A. B.; Yin, G. I.; Gibbs-Davis, J. M.; Lettan, R. B., II; Bertin, P. A.; Pike, R. C.; Nguyen, S. T.; Scheidt, K. A.; Geiger, F. M. *J. Phys. Chem. C* **2007**, *111*, 1567.
(17) Stumm, W.; Morgan, J. J. *Aquatic Chemistry, Chemical Equilibria and Rates in Natural Waters*, 3rd ed.; John Wiley & Sons: New York, 1996.
(18) Brown, G. E. *Science* **2001**, *294*, 67.
(19) Seinfeld, J. H.; Pandis, S. N. *Atmospheric Chemistry and Physics*; John Wiley & Sons: New York, 1998.
(20) Finlayson-Pitts, B. J.; Pitts, J. N., Jr. *Chemistry of the Upper and Lower Atmosphere*; Academic Press: New York, 2000.
(21) Usher, C. R.; Michel, A. E.; Grassian, V. H. *Chem. Rev.* **2003**, *103*, 4883.
(22) Morel, F. M. M.; Hering, J. G. *Principles and Applications of Aquatic Chemistry*; Wiley-Interscience: New York, 1993.
(23) Schwarzenbach, R.; Gschwend, P. M.; Imboden, D. M. *Environmental Organic Chemistry*; John Wiley & Sons: New York, 1993.
(24) Newman, D. K.; Banfield, J. F. *Science* **2002**, *296*, 1071.
(25) Torrens, J. L.; Herman, D. C.; Miller-Maier, R. M. *Env. Sci. Technol.* **1998**, *32*, 776.
(26) Frauenfelder, H. *Proc. Natl. Acad. Sci. U.S.A.* **2002**, *99*, 2479.

Scheme 1. Functionalization of Fused Quartz or Glass Surfaces with NHS-Ester Silanes and the Subsequent Amino Acid Coupling Scheme

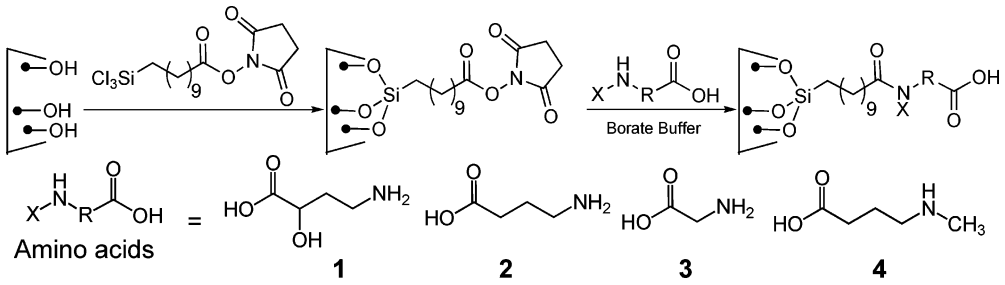

chemical events at environmental interfaces. The resulting knowledge gap adversely impacts the accuracy of climate forecasts[27] and geochemical transport models.[28]

Organic adlayers at environmental interfaces are often composed of natural organic matter,[23,29,30] humic acids,[31]or humic-like substances[32] that contain organic functional groups, such as esters, polyphenols, heterocycles, and amino acids. Carboxylic acids are especially common chemical functional motifs in humic acids.[31,33] Another major component of soil that has recently received much attention consists of peptides and larger proteinaceous materials,[31] in which the most abundant nitrogen-containing moiety is due to amide groups that form the backbone of peptides. Understanding how these functional groups control the interactions of solvated species with environmental interfaces provides detailed molecular-level insight into complex heterogeneous processes. This knowledge can result in improved transport modeling and control of environmentally relevant species in geochemistry, biology, and atmospheric science. Our approach to determining the fate of pollutants in the soil, specifically, is to track their binding interactions with important environmentally relevant functional groups, such as carboxylic acids and amide groups, at solid/aqueous interfaces. The measured thermodynamic binding constants are then applied in models that predict geochemical endpoints, such as environmental mobility and chemical transport.

In this work, we report resonantly enhanced surface second harmonic generation (SHG) measurements of the EPA priority toxic metal pollutant chromium(VI),[34−41] which is a known carcinogen, at tailor-made amino acid functionalized fused quartz/water interfaces. These interfaces serve as chemical model systems for peptide-rich natural organic matter and humic acids at mineral/water interfaces. We show that amide-containing carboxylic acids can dramatically increase the binding affinity of mineral oxide/water interfaces toward Cr(VI), with direct implications for its environmental and biological fate.

2. Experimental Section

2.1. Preparation of Amido Acid Functionalized Fused Quartz Surfaces: *N*-Hydroxysuccinimidyl (NHS) ester groups have been used extensively to covalently tether biomolecules and small molecules to the surfaces of biochips and microparticles.[42,43] Recently, we have adopted a strategy that is based on NHS-esters for generating tailor-made surfaces with a wide range of chemical properties. This strategy allows us to investigate a number of important interfaces that model environmental[16,44] and biological systems.[15] Glass and silica surfaces are functionalized in one step by exposing them for 1 h to a solution of 10-trichlorosilylundecanoic acid NHS-ester in dry toluene. The resulting electrophilic surfaces provide a platform for subsequent functionalization via reaction with nucleophiles in solution. For this investigation, various amino acids were reacted overnight with the NHS-ester functionalized fused quartz surfaces in buffer or organic solvent, resulting in amide bond formation at the amine terminus of the amino acid. Scheme 1 illustrates the procedure for preparing our functionalized interfaces and the amino acids presented herein.

(*S*)-4-Amino-2-hydroxybutyric acid, 4-aminobutyric acid, 2-aminoethanoic acid, and butylamine used in this study were purchased from Aldrich and used without further purification. The trichlorosilylundecanoic acid NHS-ester compound[15] and *N*-methyl-4-aminobutyric acid[45] were prepared according to the literature. Prior to functionalization, all fused quartz hemispheres were covered with NoChromix (1 h), rinsed with water, sonicated in methanol (6 min), rinsed with methanol (3 × 5 mL), placed in an 80 °C oven for 15 min, and cleaned for 25 s in an oxygen plasma cleaner. The surfaces were then functionalized with the NHS-ester silane according to our previously published procedure.[15] For secondary amido acid surface functionalization, an NHS-ester functionalized surface was covered with a 0.1 M solution of the primary amino acid in 0.1 M sodium borate buffer (pH = 8.5) and allowed to react overnight. For tertiary amido acid surface functionalization, the NHS-ester functionalized fused quartz surface was exposed to a 0.3 M solution of the secondary amino acid in the borate buffer and also allowed to react overnight. The surface was then rinsed with water and stored in water until further use. All surfaces were prepared within 1 week of being used. In the case of butylamine or 4-fluorobenzylamine, the NHS-ester functionalized fused quartz surface was covered in a 0.1 M solution of the amine in dry CH_2Cl_2 and allowed to react overnight. The *N*-methyl-4-fluorobenzylamine was coupled in a similar manner at higher amine concentrations (0.3 M). The surface was then rinsed with acetone or methanol and used immediately.

(27) IPCC *Climate Change 2001: The Scientific Basis. Contribution of Working Group I to the Third Assessment Report of the Intergovernmental Panel on Climate Change*; Cambridge University Press: New York, U.S.A., 2001.
(28) Volume I: The Kd Model, Methods of Measurement, and Application of Chemical Reaction Codes. In *Understanding Variation in Partiition Coefficient, Kd, Values*; United States Environmental Protection Agency: EPA 402-R-99-004A, 1999.
(29) McCarthy, J.; Zachara, J. M. **1989**, *23*.
(30) Brown, Jr., G. E.; Foster, A. L.; Ostergren, J. D. *Proc. Natl. Acad. Sci. U.S.A.* **1999**, *96*, 3388.
(31) Sutton, R.; Sposito, G. *Environ. Sci. Technol.* **2005**, *39*, 9009.
(32) Rudich, Y. *Chem. Rev.* **2003**, *103*, 5097.
(33) Allard, B. *Geoderma* **2006**, *130*, 77.
(34) Ellis, A. S.; Johnson, T. M.; Bullen, T. D. *Science* **2002**, *295*, 2060.
(35) Katz, S. A.; Salem, H. *The Biological and Environmental Chemistry of Chromium*; VCH: New York, 1994.
(36) Nieboer, E.; Jusys, A. A. Biologic Chemistry of Chromium. In *Chromium in the Natural and Human Environment*; Nriagu, J. O., Nieboer, E., Eds.; John Wiley & Sons: New York, 1988.
(37) Palmer, C. D.; Wittbrodt, P. R. *Environ. Health Persp.* **1991**, *92*, 25.
(38) Chromium. In *National Research Council (US): committee on biologic effects of atmospheric pollutants*; National Academy of Sciences: Washington, D.C., 1974; pp 125.
(39) Nriagu, J. O.; Nieboer, E. *Chromium in the Natural and Human Environments*; John Wiley & Sons: New York, 1988.
(40) Grevatt, P. C. "Toxicological Review of Hexavalent Chromium (CAS No. 18540-29-9)", Environmental Protection Agency, 1998.
(41) Costa, M.; Klein, C. B. *Crit. Rev. Toxicol.* **2006**, *36*, 155.
(42) Frey, B. L.; Corn, R. M. *Anal. Chem.* **1996**, *68*, 3187.
(43) Lahiri, J.; Ostuni, E.; Whitesides, G. M. *Langmuir* **1999**, *15*, 2055.
(44) Hayes, P. L.; Gibbs-Davis, J. M.; Musorrafiti, M. J.; Mifflin, A. L.; Scheidt, K. A.; Geiger, F. M. *J. Phys. Chem. B* **2007**, in press.
(45) McElvain, S. M.; Vozza, J. F. *J. Am. Chem. Soc.* **1949**, *71*, 896.

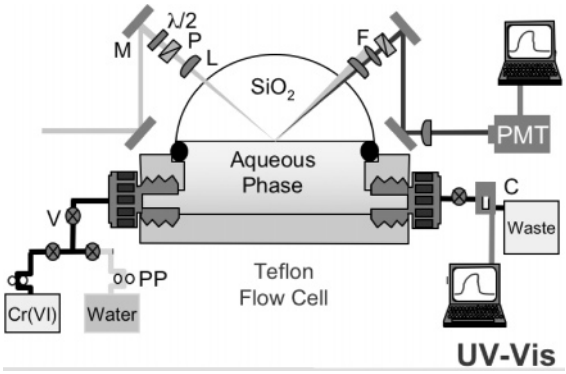

Figure 1. Pump-flow and laser system. The silica hemisphere is functionalized at the flat surface with an amido acid adlayer. M = mirror, L = lens, P = polarizer, $\lambda/2$ = half-waveplate, V = valve, PP = peristaltic pump, F = UV-grade Schott filter, C = cuvette.

2.2. Pump-Flow Setup and Laser System: The pump-flow setup is shown in Figure 1 and has been described in detail elsewhere.[46] Briefly, a fused quartz hemisphere (ISP optics) is functionalized with an amino acid or alkyl amine, placed flat side down on a custom-built Teflon flow cell, and held leak tight using a Viton O-ring. The two open ends of the flow cell are fit with Tygon tubing using Teflon Swagelok connections. The input tube is bisected using a T-joint to two more lines of tubing that are each fit through a peristaltic pump and into a reservoir filled with water or a potassium chromate (ICN) solution, respectively. This design allows us to mix the water and chromate solutions in-line prior to flowing across the sample interface. From the flow cell the output tube is connected to a flow meter and into a UV−vis cuvette for in situ monitoring of the flow rate and the bulk chromate concentration in the effluent, respectively, and finally on to the waste. The pH of the chromate and water reservoirs were adjusted to pH 7 using HCl (VWR) and/or NaOH (Spectrum Chemicals) solutions prior to the entire experiment. The flow rate was kept close to ~0.5 mL/s.

The laser system for studying chromate at environmental interfaces has been described elsewhere.[47] Briefly, we use a Ti:sapphire laser (1 kHz, 120 fs, 1 mJ/pulse, Hurricane, Spectra Physics) to pump an optical parametric amplifier (OPA-CF, Spectra Physics) tuned to 580 nm. The fundamental probe light at 580 nm is then focused through the fused quartz hemisphere at a 60° angle onto the aqueous/solid interface. The input power is attenuated to 3−4 μJ using a variable density filter, which allows for optimal signal levels that do not cause optical breakdown, as verified by the quadratic SHG intensity dependence on input power and the appropriate SHG bandwidth. The second harmonic signal generated at the interface is resonantly enhanced (vide infra) when the wavelength of the fundamental probe light approaches 580 nm because of the ligand-to-metal charge-transfer band of chromate that is centered around 290 nm when adsorbed at fused quartz/water[47] and the methyl ester functionalized fused quartz/water interfaces.[48] The output light is collected at a 60° angle after filtering out the reflected fundamental light field using a UV-grade Schott filter. The SHG signal at 290 nm is passed through a monochromator and detected using single photon counting techniques.[47]

At the beginning of each experiment, water is pumped through the flow cell and the background SHG signal intensity and the bulk solution UV−vis absorbance are recorded. Then chromate "on" traces are measured for various chromate concentrations by turning on the chromate feed and mixing it with the water pumped through the flow cell. The SHG signal intensity and the UV−vis spectrum are recorded until the SHG signal intensity levels off, i.e., until the system reaches equilibrium. The chromate feed is then turned off, and the SHG signal intensity is recorded until equilibrium is reached with the aqueous phase (water only) and no chromate is detectable in the UV−vis absorbance spectrum. To record an isotherm, the process is repeated multiple times for a single sample, generally with increasing chromate concentration at each "on"/"off" interval. All isotherms are a combination of at least two experiments, each on a different sample surface. Each experiment includes multiple submonolayer and monolayer points, and each dataset is normalized to the monolayer and then combined.

Table 1. Water Contact Angle Measurements for Various Surfaces Investigated in This Work

surface	contact angle [deg]
silica	<10
carboxylic acid	46(4)
α-hydroxy amido acid	63(3)
GABA	68(4)
glycine	64(3)
N-Me GABA	67(3)
NHS-ester	77(4)
C_{18}	96(2)

For the off-resonance interfacial potential SHG experiments (vide infra), the same experimental setup is used, but only one reservoir containing the aqueous solution is fed into the line. The aqueous solution contains 0.5 M NaCl, and the pH is adjusted with NaOH or HCl solutions. For a given bulk solution pH, the aqueous phase is flowed across the interface until the SHG signal intensity levels off, at which point the SHG signal intensity is recorded and the signal is averaged. Then the flow is temporarily stopped, the pH of the reservoir is adjusted and measured, and the aqueous phase flow is restarted until the SHG signal intensity is once again stabilized at a new level. This process is repeated multiple times for varying pH values between 3 and 12.

2.3. Contact Angle Determination: Contact angle measurements are performed using an FTA 125 Contact Angle Analyzer (First Ten Angstroms, FTA, Portsmouth VA). Glass slides are functionalized with the amino acids in the same manner as that described for the fused quartz hemisphere. The sessile volume of the water droplet was 1.9(3) μL, and the contact angle is calculated using the FTA software. The reported values are listed in Table 1 and represent the average of seven different measurements.

2.4. X-ray Photoelectron Spectroscopy (XPS) Measurements: X-ray photoelectron spectroscopy (Omicron ESCA probe, Omicron Nanotechnology) is performed on quartz slides functionalized with 4-fluorobenzylamide and *N*-methyl-4-fluorobenzylamide, respectively, prepared according to the procedures discussed above. The N 1s spectrum and F 1s spectrum are obtained at an interval of 0.040 eV and a dwell time of 0.200 s and exhibit peaks at 399.8(1) eV and 686.8-(1) eV, respectively. The coupling efficiency is calculated from the ratio of the integrated fluorine and nitrogen XPS 1s spectral intensities using sensitivity factors of 4.26 and 1.77, for F 1s and N 1s, respectively. The peak areas are determined from the peak edges that represent 10% of the peak height.

2.5. Ellipsometry: The ellipsometric measurements are taken on a multilayer optical spectrometric scanning ellipsometer (MOSS ES4G/OMA, Sopra, Inc., Menlo Park, CA) at various incident angles, and the results were analyzed using the MOSS ES4G software. The samples are prepared following the procedure described above on a glass slide as substrate. Prior to use they are rinsed with acetone and placed in an evacuated desiccator for 45 min.

2.6. Second Harmonic Generation (SHG): In an SHG experiment, a high-intensity laser pulse of frequency ω is focused at a solid/liquid interface with an energy below the damage threshold of the interface, and the SHG signal intensity generated at the interface, which oscillates

(46) Mifflin, A. L.; Gerth, K. A.; Geiger, F. M. *J. Phys. Chem. A* **2003**, *107*, 9620.
(47) Mifflin, A. L.; Gerth, K. A.; Weiss, B. M.; Geiger, F. M. *J. Phys. Chem. A* **2003**, *107*, 6212.
(48) Mifflin, A. L.; Musorrafiti, M. J.; Konek, C. T.; Geiger, F. M. *J. Phys. Chem. B* **2005**, *109*, 24386.

at half the input wavelength or twice the frequency (2ω), is monitored.[49−53] In general, the SHG signal intensity at 2ω can be related to the physical and chemical nature of the interface by the following equation:

$$\sqrt{I_{2\omega}} = E_{2\omega} \propto \chi^{(2)} E_\omega E_\omega \quad (1)$$

where $I_{2\omega}$ is the signal intensity at the second harmonic frequency, E_ω is the electric field at the input frequency, and $\chi^{(2)}$ is the macroscopic second-order susceptibility inherent to the interface. Within the electric dipole approximation, the second-order susceptibility is zero in centrosymmetric bulk media, which prevents second harmonic generation, but is nonzero at interfaces, where symmetry is necessarily broken. This surface selectivity allows us to monitor interfacial processes in situ.

$\chi^{(2)}$ can be divided into a resonant and a nonresonant term. At the fundamental and SHG wavelengths employed in this work, the nonresonant component drives the SHG background signal from the fused quartz/water interface. The resonant contribution stems from the electronic structure of the surface species and increases with the number of adsorbed molecules according to

$$\chi_R^{(2)} \propto N_{ads} \langle \beta_R^{(2)} \rangle \quad (2)$$

where $\beta_R^{(2)}$ is the orientationally averaged molecular second-order polarizability, or hyperpolarizability, of the interfacial species and N_{ads} is the number of resonators at the interface. $\beta_R^{(2)}$ becomes significant when the second harmonic frequency 2ω or the input frequency ω approaches that of an electronic transition within the surface-bound species, according to

$$\beta_R^{(2)} \propto \frac{1}{(\omega_{ba} - \omega - i\Gamma_{ba})(\omega_{ca} - 2\omega - i\Gamma_{ca})} \quad (3)$$

Here, Γ is an optical damping term. Thus, SHG resonance enhancement provides us with a molecularly specific and quantitative handle for probing adsorbates directly and in situ. By tuning the SHG wavelength to an electronic transition within the chromate anion and by using eqs 1−3, we can monitor the chromate surface coverage by changes in the SHG signal intensity as a function of chromate concentration or time.[47,54]

3. Results and Discussion

3.1. Surface Characterization: Prior to the nonlinear optical measurements, the surfaces under investigation in this work were characterized using ellipsometry, XPS, and contact angle measurements. Ellipsometry shows that the thickness of the NHS-ester functionalized organic layer, 1.9(1) nm, corresponds to the length of one NHS-ester silane molecule and thus indicates high surface coverages. This thickness does not change when the NHS-ester adlayer is reacted with γ-amino butyric acid (GABA, **2**, 1.9(2) nm). The similarity in adlayer thickness and the corresponding drop in contact angles observed after reaction (vide infra) are consistent with the displacement of the NHS group by the more flexible and only slightly longer amino acid if the resulting amide-linked acid assumes a bent, rather than extended, conformation. To assess the degree of surface conversion of NHS-esters to secondary amides via reaction with a primary amine, X-ray photoelectron spectroscopy (XPS) was performed on an NHS-ester functionalized surface that had been reacted overnight with 4-fluorobenzylamine (0.1 M). Based on the ratio of the fluorine (F 1s) to nitrogen (N 1s) peaks, 73% of the NHS groups were displaced by the 4-fluorobenzylamine. An analogous experiment was performed on an NHS-ester functionalized fused quartz surface reacted overnight with *N*-methyl-4-fluorobenzyl amine (0.3 M). According to the ratio of the peaks in the XPS trace, 67% of the NHS-esters were displaced, despite the use of a secondary amine instead of a primary amine as nucleophile. Finally, to assess the overall hydrophobicity of our functionalized fused quartz surfaces, we performed water contact angle measurements. The amido acid functionalized surfaces are less hydrophobic than the fused quartz surface functionalized with the NHS-ester (77(4)°), with all of the amido acid functionalized fused quartz surfaces generating similar contact angles (∼65°) (Table 1). It is important to note that the contact angles are higher for fused quartz surfaces functionalized with the amino acids than for alkyl-linked carboxylic acid functionalized surfaces (46°).[54]

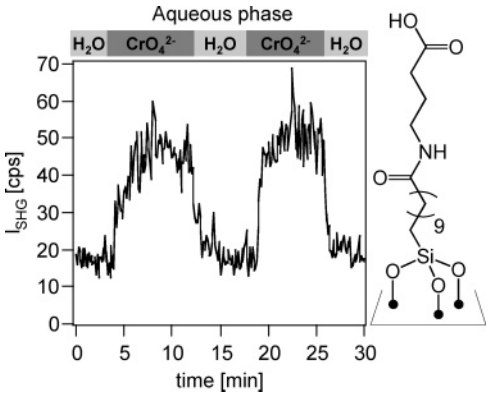

Figure 2. "On/off" traces for GABA-modified fused quartz surfaces (**2**) exposed to different chromate concentrations approaching monolayer coverages.

The somewhat hydrophobic nature of the amido acid functionalized fused quartz surface suggests that, unlike alkyl-linked carboxylic acid modified fused quartz surfaces, the aqueous phase is in contact with more than the carboxylic acid termini of the amido acid. The apparent accessibility of the aqueous phase to portions of the adlayer other than the carboxylic acid is consistent with the ellipsometry results and becomes important when considering the chromate binding mechanism at the amido acid modified fused quartz/water interface (vide infra).

3.2. Adsorption Studies Based on Resonantly Enhanced Second Harmonic Generation (RE-SHG): After characterizing the amido acid functionalized surfaces, chromate binding constants were measured directly at the aqueous/solid interface by recording the relative surface chromate coverage as a function of bulk chromate concentration using ligand to metal charge-transfer resonantly enhanced SHG.[47]

Figure 2 shows representative SHG vs time traces recorded at 290 nm for chromate interacting with the γ-aminobutyric acid (GABA) functionalized quartz/water interface. The data clearly show fully reversible chromate binding, as indicated by the return of the SHG signal intensity to the original nonresonant level after chromate exposure is ceased and water is flowed across the interface. Previous SHG work on chromate at

(49) Heinz, T. F. *Nonlinear Surface Electromagnetic Phenomena*; Elsevier Publishers, 1991.
(50) Eisenthal, K. B. *Chem. Rev.* **1996**, *96*, 1343.
(51) Shen, Y. R. *The Principles of Nonlinear Optics*; John Wiley & Sons: New York, 1984.
(52) Eisenthal, K. B. *Chem. Rev.* **2006**, *106*, 1462.
(53) Simpson, G. J.; Rowlen, K. L. *Acc. Chem. Res.* **2000**, *33*, 781.
(54) Al-Abadleh, H. A.; Voges, A. B.; Bertin, P. A.; Nguyen, S. T.; Geiger, F. M. *J. Am. Chem. Soc.* **2004**, *126*, 11126.

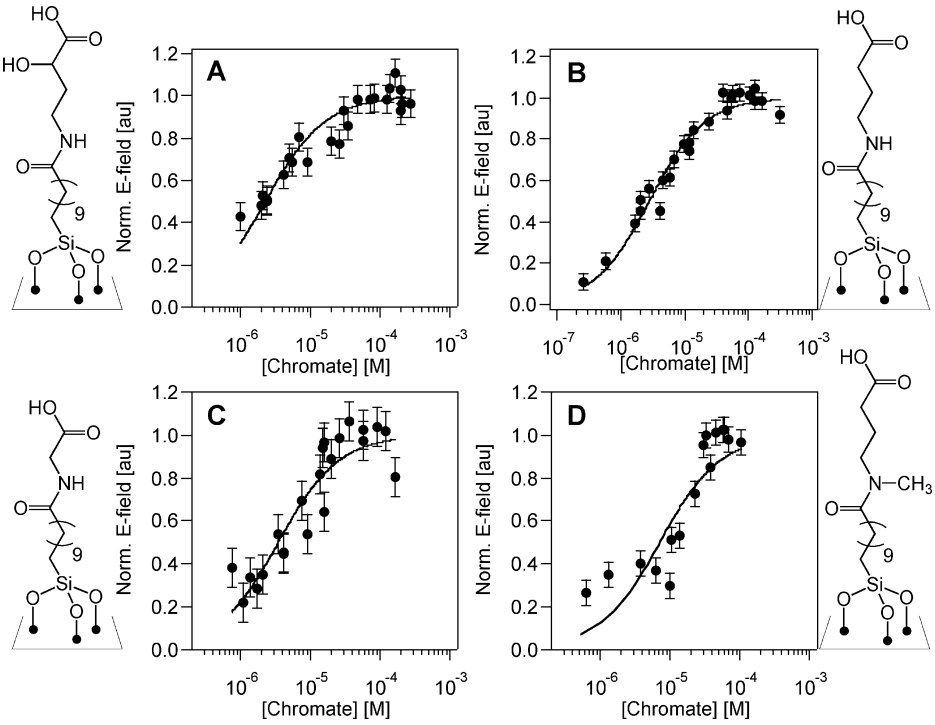

Figure 3. Chromate adsorption isotherms measured by SHG for fused quartz/water interfaces functionalized with (A) amide-linked α-hydroxy carboxylic acid, (B) amide-linked GABA, (C) amide-linked glycine, and (D) amide-linked *N*-methyl GABA. Filled circles are the measured data, and solid lines represent the Langmuir fit.

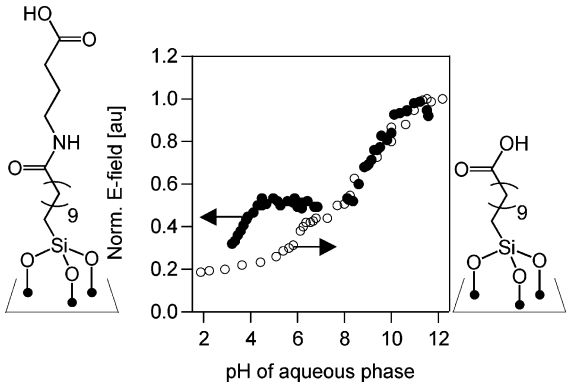

Figure 4. Normalized SHG E-field as a function of the bulk solution pH for fused quartz/water interfaces functionalized with the amide-linked GABA (●) and alkyl-linked carboxylic acids (○). The data from multiple runs were normalized to the center plateau and then divided by the maximum E-field obtained at pH 11.5.

aqueous/solid interfaces established a 90° phase difference between the nonresonant "off" intensity and the resonantly enhanced "on" intensity.[48] Thus, the resonant E-field, which is proportional to the surface coverage of chromate, can be determined from the square root of the difference in the "on/off" intensities (eq 1 and 2), clearly indicating that the order of operations matters. Tracking this difference as a function of chromate concentration yields adsorption isotherms for the various interfaces under investigation (Figure 3A−D). Control experiments show minor chromate−NHS-ester interactions, which is not surprising as the NHS group is only somewhat polar. The relative SHG E-field magnitudes found for a chromate monolayer on the NHS-ester is about 20% of the E-field magnitude found for chromate monolayers on the amido acids.

Our previous work with alkyl-linked carboxylic acids and methyl esters revealed that chromate interacted through hydrogen bonds with these functionalized fused quartz/water interfaces.[54,55] Thus, our first interest was to prepare a surface with an additional hydrogen-bonding moiety such as an α-hydroxy acid, a motif observed in soil organic matter.[33] We anticipated that the additional hydrogen-bond donor on the α-hydroxy acid would increase the binding affinity of chromate compared with the original carboxylic acid surfaces. After measuring the isotherm at pH 7 on two α-hydroxy acid functionalized samples, the normalized data set was fit to a Langmuir model that describes reversible physisorption processes by relating the binding constant (K) to the surface coverage (θ) proportional to the resonant E-field and the chromate concentration in the bulk (c):

$$\theta = \frac{Kc}{1 + Kc} \tag{4}$$

As shown in Figure 3A, the Langmuir model fits our data for the α-hydroxy acid surface (**1**) in the submonolayer and monolayer regimes fairly well. Applying the Langmuir model and referencing to the molarity of water (55.5 M), we obtained a binding constant of $3.1(2) \times 10^7$, which is 15 times greater than that observed for the alkyl-linked carboxylic acid modified fused quartz/water interface ($2.1(2) \times 10^6$).[55] To determine whether this major enhancement in binding stemmed from the presence of the α-hydroxy group or the amide moiety tethering the α-hydroxy acid to the surface, we measured the adsorption isotherm of chromate on a GABA (**2**) modified surface, which lacks the α-hydroxy moiety (Figure 3B). The Langmuir model

(55) Al-Abadleh, H. A.; Mifflin, A. L.; Bertin, P. A.; Nguyen, S. T.; Geiger, F. M. *J. Phys. Chem. B* **2005**, *109*, 9691.

agreed with the data, and from the fit the binding constant was determined to be $2.5(1) \times 10^7$. Removing the α-hydroxy moiety only had a small effect on the binding constant.

If the presence of the amide moiety alone was responsible for the increase in the binding constant with chromate, then removing the terminal carboxylic acid group should not have a significant effect on the binding. Thus, we prepared a butylamide-modified surface that is chemically identical to the GABA surface except for the substitution of the carboxylic acid group by a methyl group. The SHG signal intensity showed no appreciable increase when chromate (up to 1.3×10^{-4} M) was added to the aqueous phase and flowed across the interface, suggesting that the chromate was not interacting efficiently with the butylamide-modified surface (see Supporting Information). These results were consistent with the low to negligible binding behavior observed for chromate at alkyl-functionalized fused quartz/water interfaces[54] and indicate that amide moieties without terminal carboxylic acid groups do not promote significant chromate binding. Clearly, synergistic effects between the carboxylic acid and the amide groups are important for enhanced chromate binding, and this is discussed below.

One obvious mechanism for synergistic effects is chromate chelation by the carboxylic acid and the amide moieties of the same molecule. If this proposed chelation mechanism were to operate under the conditions of the experiment, then chromate binding should be sensitive to the length of the spacer separating the amide and the acid groups. We therefore prepared a glycine-modified surface (**3**) containing only one methylene spacer linking the amide and acid groups and measured the adsorption isotherm (Figure 3C). The binding constant for the glycine-modified surface was found to be $1.5(1) \times 10^7$, which is a factor of 2 lower than that of GABA (**2**). Evidently, chelation is optimal when several methylene units separate the amide and the terminal carboxylic acid moieties.

To test the importance of the N−H present in the amide moiety for chromate chelation, we prepared an *N*-methyl GABA amido acid functionalized (**4**) surface to eliminate the N−H group but retain the amide functionality. This structural change significantly decreased the interaction with chromate (Figure 3D), and the corresponding binding constant from the Langmuir fit was found to be $6(1) \times 10^6$. The magnitude of this binding constant is on the order of that found for the alkyl-linked carboxylic acid functionalized fused quartz/water interfaces studied in our previous work. This result suggests that the (formally) charge-separated $^-$OC═NH$^+$ moiety[56] is critical for chromate chelation. We cannot, however, rule out steric effects that prevent chelation between the *N*-methyl amide groups and chromate.

3.3. Acid/Base Properties of the GABA-Modified Surface: To further explore the molecular origin giving rise to the chromate binding differences between the amide-linked acid groups studied in this work and the alkyl-linked carboxylic acid groups studied in our previous work, we carried out pH-dependent $\chi^{(3)}$ measurements on the amido acid functionalized fused quartz/water interface. While resonantly enhanced SHG yields the electronic signatures of adsorbates, off-resonance SHG methods, such as the "$\chi^{(3)}$ technique" pioneered by Eisenthal and co-workers,[57,58] can yield important physicochemical information regarding interfacial charge densities, interfacial acid−base behavior, and interfacial energy densities. This is due to the relationship between the SHG E-field and the third-order susceptibility $\chi^{(3)}$ in the presence of a static interfacial potential, ϕ_o:

$$\sqrt{I_{2\omega}} = E_{2\omega} \approx \chi^{(2)} E_\omega E_\omega + \chi^{(3)} E_\omega E_\omega \phi_o \qquad (5)$$

Equation 5 shows that the SHG E-field is modulated by the magnitude of the interfacial potential. In the case of the amido acid functionalized fused quartz/water interfaces, the interfacial potential depends on the charge state of the amido acid groups, which, in turn, is controlled by the extent of deprotonation of the terminal carboxylic acid groups. Thus, eq 5 can be applied to obtain detailed information on the interfacial acid−base equilibria that characterize the amido acid functionalized fused quartz/water interfaces. Determining the protonation state of the surface-bound acid groups at various bulk solution pH values is critical for understanding the mechanism of how charged analytes such as chromate interact with biogeochemical systems.

Previous work, including our own, has shown that unlike carboxylic acids in solution, alkyl-linked carboxylic acid adlayers on fused quartz display two pK_a values (5.6(2) and 9(1)).[59,60] $\chi^{(3)}$ measurements show that less than 5% of the acid groups are associated with the lower pK_a value, whereas the majority of the acid groups (95%) are associated with the higher pK_a value due to stabilizing lateral hydrogen bonding interactions and the high free interfacial energies associated with the deprotonation of adjacent carboxylic acid groups.[59] The small percentage of acid groups that are deprotonated at lower pH suggests that they are located at edges or defect sites, which prevent participation in the lateral hydrogen-bonding network.[59] At pH 7, more than 90% of the carboxylic acids groups are protonated, i.e., neutral,[59] which accounts for their relatively high binding affinity toward the chromate dianion.[55]

$\chi^{(3)}$ measurements carried out at the GABA-functionalized fused quartz/water interface as a function of bulk solution pH (constant NaCl concentration) show two distinct inflection points near pH 4 and 9 (Figure 4). The lower inflection point occurs near the pK_a value measured for the acidic side chains on glutamic acid (pK_a = 4.1).[61] This pK_a value is significantly lower than that of acetic acid in water (pK_a = 4.8), which is consistent with the pK_a and p$K_{a1/2}$ values reported for the alkyl-linked carboxylic acid functionalized fused quartz/water interfaces.[59,60]

In the higher pH region, the $\chi^{(3)}$ results reported for the alkyl-linked carboxylic acid functionalized fused quartz/water interface[59] are nearly superimposable with those obtained for the GABA system. Because of the unfavorable deprotonation of the amide moiety,[62] we attribute the inflection point observed for the GABA-functionalized fused quartz/water interface at around pH 9 to the acid−base equilibrium that corresponds to the deprotonation of those carboxylic acid groups that are likely

(56) Pauling, L. *The Nature of the Chemical Bond*; Cornell University Press: Ithaca, NY, 1960.
(57) Yan, E. C. Y.; Liu, Y.; Eisenthal, K. B. *J. Phys. Chem. B* **1998**, *102*, 6331.
(58) Zhao, X. L.; Ong, S. W.; Wang, H. F.; Eisenthal, K. B. *Chem. Phys. Lett.* **1993**, *214*, 203.
(59) Konek, C. T.; Musorrafiti, M. J.; Al-Abadleh, H. A.; Bertin, P. A.; Nguyen, S. T.; Geiger, F. M. *J. Am. Chem. Soc.* **2004**, *126*, 11754.
(60) Gershevitz, O.; Sukenik, C. N. *J. Am. Chem. Soc.* **2004**, *126*, 482.
(61) Tanford, C. *Adv. Protein Chem.* **1962**, *70*, 69.
(62) Bordwell, F. G.; Fried, H. E.; Hughes, D. L.; Lynch, T. Y.; Satish, A. V.; Whang, Y. E. *J. Org. Chem.* **1990**, *55*, 3330.

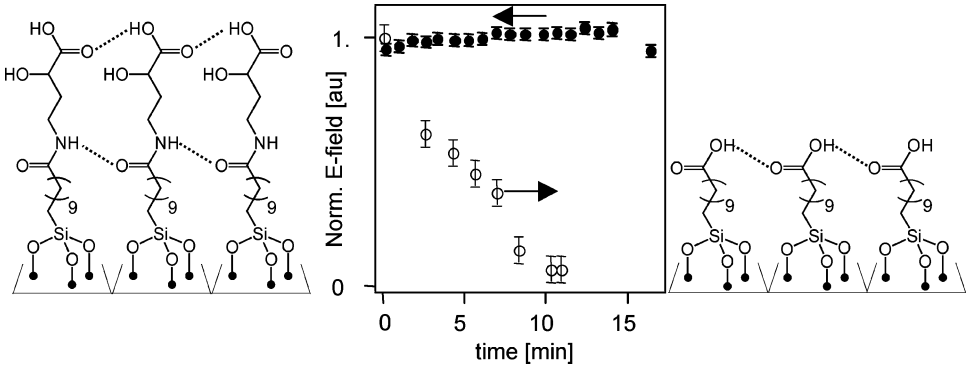

Figure 5. Normalized SHG E-field vs time trace for fused quartz/water interface functionalized with the amide-linked α-hydroxy acid (●) and with the aliphatic carboxylic acid (○) during exposure to chromate at pH = 7 (2×10^{-4} M and 1.5×10^{-4} M, respectively) and possible lateral hydrogen-bonded networks among the organic adlayers.

Table 2. Thermodynamic Data for the Amide-Linked and Alkyl-Linked Acid Modified Fused Quartz Surfaces

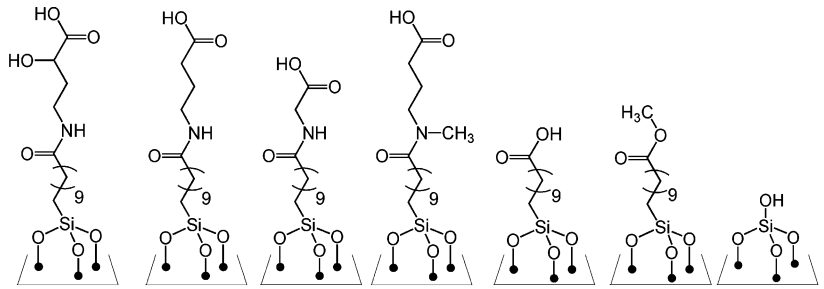

Surface	α-Hydroxy carboxylic acid	GABA	Glycine	*N*-Me GABA	Carboxylic acid[a]	Methyl ester[a]	Bare quartz[a]
K x 10^6	31(2)	25(1)	15(1)	6(1)	2.1(2)	3.2(2)	1.2(1)
ΔG_{ads} [kJ/mol][a]	-43(2)	-42(1)	-41(2)	-39(8)	-36(2)	-37(1)	-35(3)
K_d [mL/g]	0.092	0.069	0.054	0.018	0.011	0.011	0.007
R_f	1.37-1.92	1.28-1.69	1.22-1.54	1.07-1.18	1.04-1.11	1.04-1.11	1.03-1.07

[a] Thermodynamic parameters, partition coefficients, and retardation factors taken from ref 55.

to be involved in a lateral hydrogen bond network, similar to what was reported by Gershevitz and Sukenik.[60]

Because of the two negative charges on the chromate anion, chromate binding is not believed to occur at the deprotonated carboxylic acid groups but at those sites that remain protonated, i.e., neutral. The similarity of the more alkaline acid−base equilibrium for the alkyl-linked and the amide-linked carboxylic acid functionalized fused quartz/water interfaces suggests that the interaction of chromate with the carboxylic acid groups occurs in the same type of laterally hydrogen-bonded environment. The increased chromate binding constants for the case of the amido acid functionalized fused quartz/water interfaces indicate that chromate chelation by the amide and carboxylic acid moieties can still occur efficiently in this environment.

3.4. Stability: While working with the alkyl-linked carboxylic acid functionalized fused quartz/water interfaces, we observed major SHG signal intensity decreases after only half an hour of constant exposure to chromate.[55] This intensity decrease was attributed to chromate penetrating the adlayer and oxidizing the siloxane, leading to a disordered adlayer and therefore less SHG signal intensity. In contrast to these results, Figure 5 illustrates the effect on the SHG signal intensity obtained from the amide-linked α-hydroxy acid (**1**) functionalized fused quartz/water interface during prolonged exposure to 0.2 mM chromate. For nearly 3 h of chromate exposure, the signal remained stable and appreciable signal intensity decreases were not observed.

The enhanced stability of the amido acid surfaces is likely due to the stabilizing hydrogen lateral bonding interactions among the neighboring amide groups (Figure 5), which may prevent penetration of the chromate into the organic adlayer and subsequent oxidation of the siloxane. This scenario is reminiscent of interactions in β-sheet secondary structures of proteins[63] and is consistent with recent reports by Lewis et al.,[64] Song et al.,[65] and Sek et al.,[66] who reported similar stabilities for amide-linked alkyl monolayers when exposed to basic media. The stability gained from the introduction of amide groups in

(63) Voet, D.; Voet, J. G. *Biochemistry*, 3rd ed.; Wiley Text Books: New York, 2004.
(64) Lewis, P. A.; Smith, R. K.; Kelly, K. F.; Bumm, L. A.; Reed, S. M.; Clegg, R. S.; Gunderson, J. D.; Hutchison, K. E.; Weiss, P. S. *J. Phys. Chem. B* **2001**, *105*, 10630.

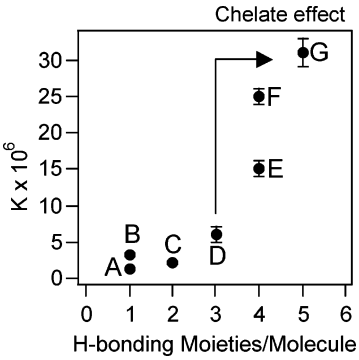

Figure 6. Chromate binding constants as a function of hydrogen-bonding moieties per silane molecule. For simplicity, only carbonyl moieties were counted as H-bond acceptors. The chromate binding constant for the bare silica/water interface is included for comparison. A = fused quartz; B = carboxylic acid; C = methyl ester; D = *N*-methyl GABA; E = Glycine; F = GABA; G = α-hydroxy carboxylic acid.

organic adlayers and self-assembled monolayers is clearly noteworthy in the context of materials synthesis and rational surface modification.

The high affinity of amido acid functionalized fused quartz surfaces toward chromate and the high stability of amido acid motifs in the presence of chromate suggest a possible mechanism for Cr(VI) transport across cell membranes, an area which remains relatively unknown.[36,41,67,68] Transmembrane proteins that are commonly displayed to the extracellular environment could bind incoming chromate and thereby increase the local concentration at the extracellular interface. High local chromate concentrations associated with amino carboxylic acids or amide moieties of mobile membrane proteins could then facilitate membrane ion transport similar to the mechanism suggested for siderophore-mediated iron transport in microbes.[69]

4. Implication of Thermodynamic Parameters on the Mechanism of Binding and Environmental Endpoints

The thermodynamic and mechanistic evidence presented in the previous sections suggests that the interactions of chromate with the interfaces under investigation in this work are driven by hydrogen-bonding interactions. Table 2 shows the chromate binding constants and the free adsorption energies obtained from the Langmuir model fits to the experimentally determined adsorption isotherms for the bare fused quartz/water interface (no organic adlayers present) and those interfaces functionalized with the amido acids and the aliphatic acid and methyl ester studied in our previous work.[55] With the exception of the *N*-Me GABA (**4**) surface, the chromate binding constants obtained for the amido acids are found to be an order of magnitude higher than those for the other interfaces. The large chromate binding constants associated with the amide-containing organic adlayers are attributed to the chelating ability of the amido acid groups presented to the incoming chromate ion.

To demonstrate the possibility of a chelation mechanism quantitatively, we plotted the chromate binding constants against the number of H-bond donor and acceptor moieties for each silane molecule under investigation (Figure 6). While the chromate binding constants are found to be relatively low for organic adlayers containing up to three H-bonding moieties per silane molecule, substantial increases in the chromate binding constants occur for four and more H-bonding moieties. This finding is consistent with a chelation mechanism that involves multiple hydrogen-bond donors and/or acceptors at those surfaces that contain a high density of optimally spaced H-bonding groups. In this analysis, we count three or four H-bonding moieties for *N*-methyl GABA but plot the binding constant for only three H-bonding moieties; counting four would make the onset of the chelate mechanism even sharper.

The observation that amide groups increase the chromate binding constant by an amount that corresponds to a free energy difference of up to 6 kJ/mol is consistent with the presence of an additional hydrogen bond between the chromate (or water-solvation sphere) and the amide N−H bond, which has been reported to be associated with free energy changes of around 8 kJ/mol.[70] Our observation that the chromate binding constant decreases by a factor of 4 upon replacement of the N−H group with an *N*-methyl group (vide supra) further indicates that the chelation effect is likely to involve the N−H bond as opposed to the amide-carbonyl group. Clearly, the dipolar nature of the $^{-}$OC=NH^{+} moiety is important as well. It is interesting to note that this enhanced binding associated with the interaction of chromate with amide-linked surfaces is not observed in the case of oxytetracycline, an antibiotic used as a feed-additive in industrial farm animals.[44] Oxytetracycline is significantly larger than chromate and has a more complicated configuration as opposed to the tetrahedral geometry of the chromate dianion. Most importantly, oxytetracycline can undergo hydrophobic interactions with surfaces and interfaces, whereas this is not expected for the chromate anion.

The chelation mechanism was further investigated by comparing a single-site and a dual-site Langmuir adsorption model. The single-site Langmuir model assumes reversible interactions between an adsorbate and *one* binding site on the surface. For single binding sites containing multiple chelating groups, the chelation mechanism would occur in an intramolecular fashion. In contrast, if chelation were to occur intermolecularly, involving for instance one amide group on one silane molecule and one carboxylic acid group on a neighboring silane molecule, then the single-site Langmuir model should be replaced by the dual-site Langmuir model. The applicability of the single-site vs the dual-site Langmuir adsorption model can be tested in a straightforward manner:[71,72] the single site adsorption model will result in a linear relationship between inverse surface coverage θ (proportional to the inverse E-field) and inverse chromate concentration c. In contrast, the dual-site Langmuir model will result in a linear relationship between $[1 - (1 - \theta)(2Kc)]^2$ and chromate concentration. Figure 7 shows the results from this analysis for the interaction of chromate with the GABA-functionalized fused quartz/water interface. When applying the dual-site Langmuir adsorption model, the data set does not follow a linear relationship with the proper slope ($4K$) for a variety of K values, indicating that the binding interaction can

(65) Song, S.; Ren, S.; Wang, J.; Yang, S.; Zhang, J. *Langmuir* **2006**, *22*, 6010.
(66) Sek, S.; Palys, B.; Bilewicz, R. *J. Phys. Chem. B* **2002**, *106*, 5907.
(67) Aaseth, J.; Alexander, J.; Norseth, T. *Acta Pharm. Toxicol.* **1982**, *50*, 310.
(68) Alexander, J.; Aaseth, J. *Analyst* **1995**, *120*, 931.
(69) Stintzi, A.; Barnes, C.; Xu, J.; Raymond, K. N. *PNAS* **2000**, *97*, 10691.
(70) Jeffrey, G. A. *An Introduction to Hydrogen Bonding*; Oxford University Press: New York, 1997.
(71) Masel, R. I. *Principles of Adsorption and Reaction on Solid Surfaces*; John Wiley & Sons: New York, 1996.
(72) Atkins, P. W. *Physical Chemistry*, 6th ed.; Oxford University Press: Oxford, New York, 1998.

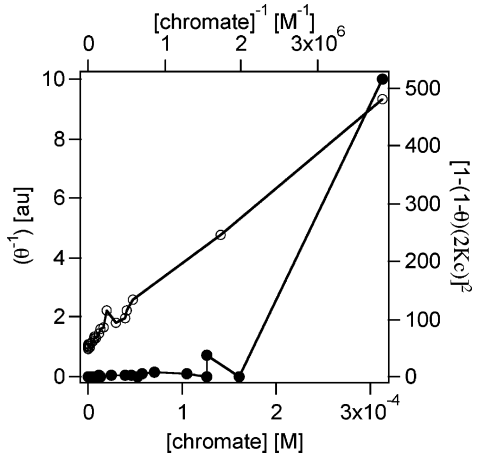

Figure 7. [SHG-E field]$^{-1}$ vs [chromate]$^{-1}$ (○) and $[1 - (1 - \theta)(2Kc)]^2$ vs [chromate] ($K = 25 \times 10^6/(55.5\ \text{M})$) (●), respectively, for chromate interaction with the GABA-functionalized fused quartz/water interface. Only the E-field^{-1} vs [chromate]$^{-1}$ follows a linear relationship.

be represented by a single-site Langmuir adsorption model. Thus, the single-site binding model that is consistent with the data presented in Figure 7 suggests that chromate binding occurs intramolecularly.

Intramolecular chelation is consistent with the fact that the glycine-functionalized fused quartz/water interface displays a lower binding constant ($15(1) \times 10^6$; see Table 2) than the GABA-functionalized fused quartz/water interface ($25(1) \times 10^6$). Intermolecular chelation would have been expected to result in the same binding constants, irrespective of the structural difference between glycine and GABA, which consists of two methylene groups between the carboxylic acid terminus and the amide group. Chromate is thus thought to interact with the various H-bond donors and acceptors within a given silane molecule. However, these interactions are not strictly additive, as demonstrated by the nonlinear relationship between the number of H-bonding moieties in the silanes and the chromate binding constants (Figure 6). This nonlinearity strongly suggests multivalent interactions between each chromate molecule and the surface site.

The interactions of aqueous chromate with the amido acid modified fused quartz/water interfaces studied in this work can be used to model the mobility of chromate in heterogeneous geochemical environments containing insoluble natural organic matter rich in peptides and carboxylic acids. Geochemical transport modeling is an important environmental endpoint as it has direct implications for influencing environmental policy.[73] Using the straightforward Kd model, which compares the flow rate of a pollutant to that of groundwater, the effect of chromate adsorption processes on the transport rate can be quantitatively assessed. While the model limitations are substantial,[55,73] the K_d parameter is easily calculated and represents the partitioning of chromate between the solution and the interface. Following our previously published protocol for obtaining K_d values from adsorption isotherms,[46] the retardation factor (R) for chromate with respect to groundwater flow can be determined for a range of soil porosities from

$$R = 1 + \frac{\rho}{n} K_d \qquad (6)$$

where ρ and n are the soil density and the porosity, respectively. Using the typical range of values for ρ/n (4−10),[74] we determined the K_d values from the adsorption isotherms for chromate interacting with the various interfaces under investigation. The results are listed in Table 2 along with the corresponding retardation factors calculated from eq 6. The large differences in the K_d and R values for chromate transport across plain quartz/water interfaces versus chromate transport across aqueous/solid interfaces containing peptide-containing organic matter in soil clearly indicate that amido acid groups in natural organic matter, including humic acids, can greatly control chromate transport in the environment. These results are an important contribution to resolve conflicting results from environmental field studies as to whether or not organic matter affects the chromate retardation.[75] Ignoring the binding contribution of peptide groups, which are abundant in humic acids, would significantly underestimate the geochemical residence time of chromate and lead to overestimates of chromate transport rates, with direct implications for environmental cleanup and policy decisions at the federal and state levels.

5. Conclusions

Resonantly enhanced second harmonic generation has allowed us to track the interaction of chromate with amino acid functionalized aqueous/solid interfaces. To understand the role of chemical complexity in soil organic matter, we applied organic chemistry to generate surfaces with complex functional groups that abound in the natural environment. Amido acid functionalized fused quartz surfaces are useful models for not only environmental but also biological interfaces. The multivalent functionalized fused quartz/water interfaces enabled us to assess the mobility, and thus the fate, of chromate in heterogeneous geochemical and biological environments quantitatively and from a mechanistic perspective. The experimental results from this work are consistent with an intramolecular chelation mechanism for chromate interaction with amido acid functionalized aqueous/solid interfaces that becomes important when a given surface-bound amino acid displays three or more hydrogen-bonding moieties toward the incoming chromate. The strong binding affinities of the amido acid functionalized fused quartz/water interfaces toward chromate result in transport rates that are nearly 50% slower than the rate of groundwater, indicating that, in the absence of redox processes, peptide materials in natural organic matter can significantly affect the residence time of chromate contamination plumes, particularly when compared with bare silica rich in aliphatic carboxylic acids. Finally, $\chi^{(3)}$ measurements show that amido acid functionalized fused quartz/water interfaces exhibit two pK_a values, as was observed for the alkyl-linked acids. This similarity suggests that, despite the chemical differences between amino acids and aliphatic carboxylic acids, both form strong laterally hydrogen-bonded networks.

The strong evidence for synergistic effects dominating the interactions of chromate with organic matter, which is highly

(73) Understanding Variation in Partition Coefficient, K_d, Values: Introduction. In *www.epa.gov/radiation/cleanup/partition.htm*; United States Environmental Protection Agency, 2003; Vol. www.epa.gov/radiation/cleanup/partition.htm.

(74) Langmuir, D. *Aqueous Environmental Geochemistry*; Prentice Hall, Inc: New Jersey, 1997.

(75) Understanding Variation in Partition Coefficient, K_d, Values: Appendix E, Partition Coefficients for Chromium (VI); United States Environmental Protection Agency, 2003; Vol. www.epa.gov/radiation/cleanup/partition.htm.

dense in multivalent functional groups, indicates that the chemical complexity in the system can be systematically addressed using tailor-made organic surfaces and interfaces. Our synthetic strategy allows for the introduction of such complexity into the various organic adlayers under investigation. Future work will include the generation of surfaces modified with highly functional amino acid residues and peptides and will focus on their acid/base properties as well as their affinity for other analytes of environmental and biological concern.

Acknowledgment. J.M.G.-D. gratefully acknowledges a fellowship from the Camille and Henry Dreyfus Postdoctoral Program in Environmental Chemistry. The XPS measurements were performed at the Northwestern University Keck II/NUANCE facility, and we are grateful to Prof. R. P. H. Chang for use of the ellipsometer. This work is supported by the National Science Foundation through the CAREER program in Experimental Physical Chemistry. We also gratefully acknowledge support from the Chemical Sciences, Geosciences and Biosciences Division, Office of Basic Energy Sciences, Office of Science, U.S. Department of Energy, the DOE-funded Northwestern University Institute for Environmental Catalysis, the Northwestern University International Institute for Nanotechnology, the American Chemical Society Petroleum Research Fund, and Schlumberger Oilfield Chemical Products. K.A.S. and F.M.G. are both Sloan Fellows, and F.M.G. is a Dow Chemical Company professor.

Supporting Information Available: Control experiment showing negligible Cr(VI) binding to butyl amide modified fused quartz/water interfaces. This material is available free of charge via the Internet at http://pubs.acs.org.

JA068117W